Application to optical components of dielectric porous silicon multilayers

C. Mazzoleni and L. Pavesi

Citation: Applied Physics Letters **67**, 2983 (1995); doi: 10.1063/1.114833
View online: http://dx.doi.org/10.1063/1.114833
View Table of Contents: http://scitation.aip.org/content/aip/journal/apl/67/20?ver=pdfcov
Published by the AIP Publishing

Application to optical components of dielectric porous silicon multilayers

C. Mazzoleni and L. Pavesi[a)]
I.N.F.M. and Dipartimento di Fisica, Università di Trento, via Sommarive 14, I-38050 Povo, Trento, Italy

(Received 14 June 1995; accepted for publication 7 September 1995)

Narrow-band color filters have been integrated on porous silicon layers. Distributed Bragg reflectors and Fabry–Pérot interference filters based on layered porous silicon samples are demonstrated. The effects of narrowing and tuning the porous silicon emission band are shown in structures composed by Fabry–Pérot filters integrated on top of thick porous silicon layers. © *1995 American Institute of Physics.*

The hope of a photonic entirely based on silicon has been renewed since the observation of room-temperature visible emission in porous silicon (*p*-Si).[1] The condition to reach such a goal is the development of light emitting diodes with as much electroluminescence quantum efficiency as for the photoluminescence itself. Applications could then be envisaged in several fields such as silicon flat displays. To this end, the control of the emission wavelength and the spectral narrowing of the large emission band of *p*-Si are crucial. These are possible by using interferential filters and/or narrow-band reflectors formed by dielectric films. Several examples have been proposed,[2] among which we focalize on distributed Bragg reflectors and Fabry–Pérot (F–P) filters. Distributed Bragg reflectors are narrow-band dielectric mirrors obtained by stacking periodically two layers of a high refractive index (layer H) and a low refractive index (layer L) material whose thickness is $\lambda/4$, where λ is the wavelength, measured in the material, at which the reflectance is maximum. Dielectric Fabry–Pérot filters are generally obtained by inserting a $\lambda/2$ layer in between two symmetric Bragg reflectors. The interference of the reflections of the two Bragg reflectors causes a maximum of transmission at λ (F–P mode) between two spectral regions of high reflectance (stop bands). In this letter we demonstrate the realization of high quality distributed Bragg reflectors and of Fabry–Pérot filters integrated in *p*-Si.

The use of multilayered structures formed by *p*-Si has already been suggested and demonstrated.[3,4] Multilayers of *p*-Si are possible because: (i) the etching process is self-limited (once a porous layer is formed, the electrochemical etching of this layer stops); (ii) the etching occurs mainly in correspondence of the pore tips; (iii) the porosity depends only on the current density once the other etching parameters are kept fixed; and (iv) the refractive index of *p*-Si, *n*, depends on its porosity. Therefore, by varying the current density during the etch, it is possible to vary the porosity in the etching direction. In this way, the current versus time profile is transferred in a porosity, i.e., *n*, versus depth profile.

Our procedure to obtain *p*-Si was described in Ref. 5. Briefly, the starting materials were B-doped Si wafers with a resistivity of 0.01 Ω cm. We used an aqueous HF-ethanol electrolyte with 15% concentration of HF. This HF concentration was chosen because of the large porosity variation obtained by varying the current. Indeed porosities between 42% and 83% were obtained by increasing the current density between 1 and 200 mA/cm^2. For similar current variations, the porosity changed only between 71% and 87% for a 10% HF concentration, and between 45% and 70% for a 20% HF concentration. The porosity *P*, was measured through gravimetric techniques. The samples were characterized by normal incidence reflectance measured through a monochromatized 1000 W Xe lamp and carefully normalized with respect to the known reflectance of an Al coated mirror. The luminescence was excited in a true backscattering geometry, by the 488 nm line of a 100 mW air-cooled Ar^+ laser and analyzed by a single monochromator (0.5 m focal length) followed by a cooled avalanche Ge photodiode interfaced to a computer through a lock-in amplifier.

The refractive index of thick *p*-Si samples was determined as a function of the porosity and of the wavelength, through reflectance measurements. By recording the spectral position of the interference fringes of the reflectance and through[2]

$$n=\frac{1}{2d}\left(\frac{1}{\lambda_r}-\frac{1}{\lambda_{r+1}}\right)^{-1}, \tag{1}$$

where d is the porous layer thickness and λ_r the wavelength of the rth fringe, the refractive index was determined. Typical values are reported in Table I. The etch rates of thick *p*-Si samples were determined by measurements of the depth of the hole left after dissolution of the *p*-Si layer with a 3% KOH-aqueous solution. A Solan Dektak II profilometer with a resolution of 50 nm was used. The results averaged over various thicknesses and for three different porosities are reported in Table I.

After several trials, we realized that the so-determined refractive indexes and etching rates are modified in presence of a multilayer structure. This is probably due to current focusing and defocusing effects when layers of different po-

TABLE I. Porosity *P*, current density *J*, etch rate, and refractive index *n*. *P* is measured by gravimetric techniques and *n* is given at 600 nm.

		Etch rate		
P (%)	*J* (mA/cm^2)	Thick sample (μm/s)	Multilayer sample (μm/s)	*n*
53	25.0	0.021	0.015	2.24
62	49.7	0.035	0.021	1.74
75	82.8	0.055	0.040	1.37

[a)]Electronic mail: pavesi@science.unitn.it

 0003-6951/95/67(20)/2983/3/$6.00

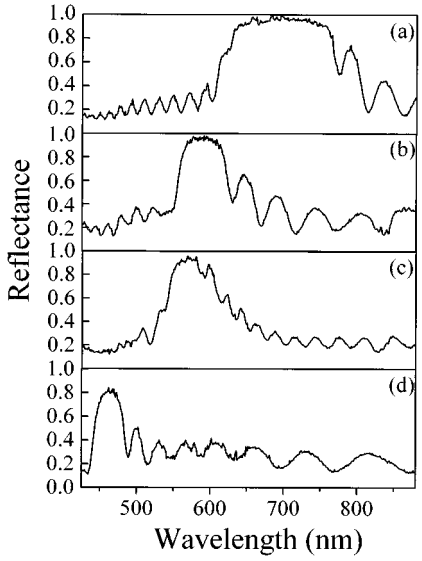

FIG. 1. Room-temperature normal incidence reflectance spectra of various Bragg reflectors (BR). Panel (a) refers to a BR centered to a wavelength (λ) of 670 nm and made by 15 repetitions of two layers of 53% and 75% porosities, respectively. Panel (b) refers to a BR centered at λ=590 nm and made by 15 repetitions of 62%–75% porosity layers. Panel (c) refers to a BR with the same structure as that of panel (b) but a larger number of repetitions: 30. Panel (d) refers to a BR centered at λ=465 nm and made by 15 repetitions of 62%–75% porosity layers.

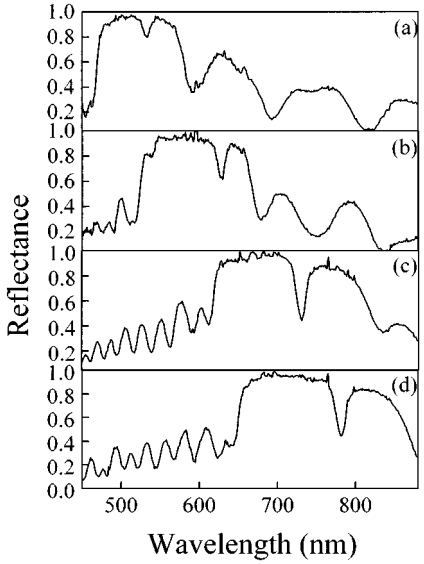

FIG. 2. Room-temperature normal incidence reflectance spectra of various Fabry–Pérot filters (F–P) of whom some characteristics are reported in Table II. All the F–P have a symmetric structure made by two Bragg reflectors (BR) separated by a λ/2 thick central layer of 75% porosity. λ is the wavelength of the F–P transmittance wavelength. Panel (a) refers to a F–P with λ=533 nm and with BR formed by 8 repetitions of two λ/4 thick layers of 62% and 75% porosities, respectively. Panel (b) refers to a F–P with λ=629 nm and with BR formed by 8 repetitions of 62%–75% porosity λ/4 layers. Panel (c) refers to a F–P with λ=731 nm and with BR formed by 6 repetitions of 62%–75% porosity λ/4 layers. Panel (d) refers to a F–P with λ=782 nm and with BR formed by 6 repetitions of 62%–75% porosity λ/4 layers.

rosities are grown on top of each other. For this reason, n and the etch rate V, of a given porosity film in the presence of a multilayer structure was measured by growing Fabry–Pérot filters and looking at the angle dependence of the wavelength of the transmittance maximum λ:

$$\lambda = 2nd\left[1-\left(\frac{\sin\phi}{n}\right)^2\right]^{1/2}, \tag{2}$$

where n and d refer to the layer between the two Bragg reflectors which constitute the F–P filter, and ϕ is the angle with respect to the normal to the surface. From the least-square fits of the experimental data with Eq. (2), both nd and n can be determined separately and, therefore, by knowing the etching time V. We found that the n and V values are systematically lower than the values determined for a thick film of the same porosity, i.e., obtained with the same current. For example, for a 53% porosity layer we measured $n=1.64$ at 714 nm and $V=0.018$ μm/s while for a thick film $n=1.95$ and $V=0.021$ μm/s. These results, i.e., lower n and V in multilayers than in thick samples, have been systematically observed. However, the characterization of several different porosity films by using this method is very time consuming and what is important for the modeling of F–P filters and Bragg reflectors is the product nd. Consequently, we have decided to use n as determined from the reflectance measurements on thick samples and to modify V according to the results of F–P resonance wavelength measurements at normal incidence where $\lambda=2nd$. The results of such determination are given in Table I.

By using n and etch rate so determined, and modeling the multilayered structures using well-known equations,[2] we were able to produce several Bragg reflectors and F–P filters. Some examples are reported in Figs. 1 and 2. The effect of variation of λ, the central wavelength of the Bragg reflectors is shown in Fig. 1. The reflectance maximum increases from 0.8 to 0.95–0.97 for increasing λ. The best results are reached for Bragg reflectors centered at long wavelengths. This is due to an increased absorbance of the p-Si layers at short wavelength, an effect which was not taken into account for the modelization of the structure. Other parameters have also been changed. The number of repetitions of the LH stacks in the Bragg reflector should be optimized with respect to the beneficial effect of an increased reflectance for a large number of repetitions and the detrimental effects of a depth dishomogeneity in the porosity for the first layers due to the effect of a long residence in the electrolyte. We have found that a good compromise is reached for a number of repetitions of 15. Compare Figs. 1(b) and 1(c). The width of

TABLE II. Parameters for the various Fabry–Pérot filters shown in Fig. 2. λ is the F–P wavelength, Δλ the width of the transmittance peak, and T_{max} its value. n_H/n_L is the ratio between the refractive indexes of the low and high porosity layers in the Bragg reflectors whose number of repetitions is indicated in the last column.

Sample	λ (nm)	Δλ (nm)	Finesse	T_{max}	n_H/n_L	Repetition No.
902	533	13	41	0.20	1.7	8
904	629	16	45	0.37	1.60	8
908	731	16	45	0.56	1.50	6
906	782	18	46	0.55	1.43	6

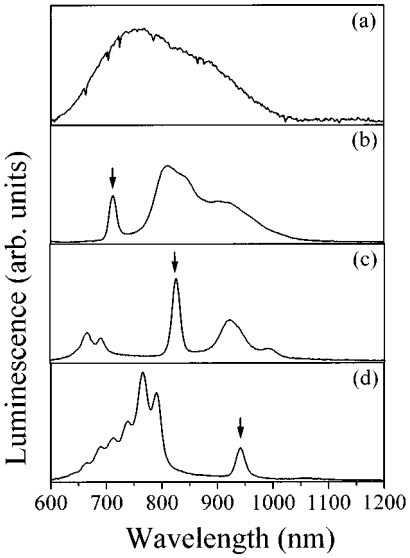

FIG. 3. Room-temperature normal incidence photoluminescence spectra of *p*-Si samples. Panel (a) refers to a 5 μm thick 75% porosity sample. Panel (b) refers to a sample constituted by a Fabry–Pérot filter (F–P) centered at 710 nm on top of a 5 μm thick 75% porous layer. The F–P finesse is 46. Panel (c) refers to a F–P centered at 828 nm and with a finesse of 49 on top of a 2 μm thick 75% porous layer. Panel (d) refers to a F–P centered at 941 nm and with a finesse of 47 on top of a 2 μm thick 75% porous layer. The arrows indicate the F–P λ. All the F–P have the same structure formed by two equal Bragg reflectors separated by a $\lambda/2$ thick and 53% porosity central layer. The Bragg reflectors are made by 6 repetitions of two $\lambda/4$ thick layers of 53% and 75% porosities, respectively. The F–P finesse has been determined by independent reflectance measurements.

the high reflectance region is determined by the refractive index difference between the H and L layers. Higher is the difference and larger is the width. An example is also shown in Figs. 1(a) and 1(b) where the ratio at λ of the refractive indexes changes from 1.52 to 1.27.

Some examples of F–P filters are reported in Fig. 2, where we have used a $\lambda/2$ thick central layer sandwiched between two equal Bragg reflectors with 6 or 8 repetitions of the $\lambda/4$ thick LH stacks. Decreasing the number of repetitions from 8 to 6 does not decrease markedly the reflectance of the stop bands while it increases the transmittance in the F–P mode (see Table II). The finesse $\mathscr{F}$ of the filters has been estimated from the normal incidence reflectance by using $\mathscr{F}=\lambda/\Delta\lambda$, where $\Delta\lambda$ is the width of the transmittance peak.[2]

The filtering effect of these F–P filters on the emission band of *p*-Si is demonstrated in Fig. 3. A comparison of the room-temperature photoluminescence spectra of a 5 μm thick 75% porosity *p*-Si sample with those of samples constituted by a F–P filter on top of a thick (some μm) 75% porosity *p*-Si layer, is performed. The wide emission band of *p*-Si is strongly narrowed by the action of the F–P filter. We also note an enhancement of the photoluminescence. In addition, by tuning the F–P wavelength λ it is possible to select the emission wavelength of the structure. In Fig. 3, the sideband emissions are due to the narrow stopbands of the Bragg reflectors. The width of the stopband can be increased by increasing the refractive index mismatch between the layers forming the Bragg reflectors.

In conclusion, we have demonstrated the feasibility of both wavelength selection and narrowing of the emission band of *p*-Si layer by using F–P filters integrated on top of thick emitting *p*-Si layers. This opens interesting possibilities in the application of light emitting silicon.

We acknowledge W. Theiss for helpful discussions and for providing us with the refractive index and reflectance simulation program SCOUT. This work has been supported by the Italian National Council of Research (CNR) in the framework of the L.E.S. Program.

[1] *Optical Properties of Low Dimensional Silicon Structures*, edited by D. C. Benshael, L. T. Canham, and S. Ossicini, NATO ASI Series Vol. 244 (Kluwer Academic, Dordrecht, 1993); *Light Emission from Silicon*, J. Lumin. **57** (1993); *Porous Silicon*, edited by Z. C. Feng and R. Tsu (World Scientific, New York, 1995); *Porous Silicon Science and Technology*, edited by J.-C. Vial and J. Derrien (Les Editions de Physique, Les Ulis, 1995); *Porous Silicon and Related Materials*, special issue of Thin Solid Films **255** (1995).
[2] H. A. MacLeod, *Thin-Film Optical Filters* (Adam Hilger, London, 1969).
[3] G. Vincent, Appl. Phys. Lett. **64**, 2367 (1994).
[4] M. G. Berger, C. Dieker, M. Thonissen, L. Vescan, H. Luth, H. Munder, W. Theiss, M. Wernke, and P. Grosse, J. Phys. D **27**, 1333 (1994); M. G. Berger, M. Thonissen, R. Arens-Fisher, H. Munder, H. Lutz, M. Arntzen, and W. Theiss, Thin Solid Films **255**, 313 (1995).
[5] L. Pavesi, M. Ceschini, G. Mariotto, E. Zanghellini, O. Bisi, M. Anderle, L. Calliari, M. Fedrizzi, and L. Fedrizzi, J. Appl. Phys. **75**, 1118 (1994).